

# Multimodal Survival Modeling in the Age of Foundation Models

Steven Song<sup>1,2,3,6,✉</sup>, Morgan Borjigin-Wang<sup>1,4,6</sup>, Irene Madejski<sup>1,2</sup>, and Robert L. Grossman<sup>1,2,5,7,✉,\*</sup>

<sup>1</sup>Center for Translational Data Science, University of Chicago, Chicago IL

<sup>2</sup>Department of Computer Science, University of Chicago, Chicago IL

<sup>3</sup>Medical Scientist Training Program, Pritzker School of Medicine, University of Chicago, Chicago IL

<sup>4</sup>Google, Chicago IL

<sup>5</sup>Section of Biomedical Data Science, Department of Medicine, University of Chicago, Chicago IL

<sup>6</sup>These authors contributed equally

<sup>7</sup>Lead contact

\*Correspondence: rgrossman1@uchicago.edu

## SUMMARY

The Cancer Genome Atlas (TCGA) has enabled novel discoveries and served as a large-scale reference through its harmonized genomics, clinical, and image data. Prior studies have trained bespoke cancer survival prediction models from unimodal or multimodal TCGA data. A modern paradigm in biomedical deep learning is the development of foundation models (FMs) to derive meaningful feature embeddings, agnostic to a specific modeling task. Biomedical text especially has seen growing development of FMs. While TCGA contains free-text data as pathology reports, these have been historically underutilized. Here, we investigate the feasibility of training classical, multimodal survival models over zero-shot embeddings extracted by FMs. We show the ease and additive effect of multimodal fusion, outperforming unimodal models. We demonstrate the benefit of including pathology report text and rigorously evaluate the effect of model-based text summarization and hallucination. Overall, we modernize survival modeling by leveraging FMs and information extraction from pathology reports.

## KEYWORDS

multimodal survival modeling, foundation models, text summarization, pathology reports, biomedical embeddings, TCGA

## INTRODUCTION

The Cancer Genome Atlas (TCGA) has been the premier cancer research resource for nearly two decades<sup>1</sup>. Throughout its history, its harmonized data<sup>2</sup> has enabled novel discoveries through its multitudes of molecular genetic data<sup>3</sup>, histopathological images, and clinical descriptors for over 11 thousand cases across 33 cancer types. One clinical outcome that has been well studied using TCGA is cancer survival<sup>4–6</sup>.

There have been numerous studies to date that have trained bespoke models to predict patient survival from the TCGA. These models have covered a wide range in the specific cancer types studied, the data modalities used as predictive features, and the model types trained. Some have leveraged histology images<sup>7,8</sup> or RNA sequencing (RNAseq)<sup>9–12</sup> alone, while others have explored varying degrees of multimodal integration<sup>13–21</sup>. Most recent papers focus on training bespoke deep-learning models<sup>7–11,15–17,19–21</sup> and some apply simpler machine learning models<sup>12,14,18</sup>, however few explore the synergy of combining deep learning with simpler statistical, machine learning models<sup>13</sup>.

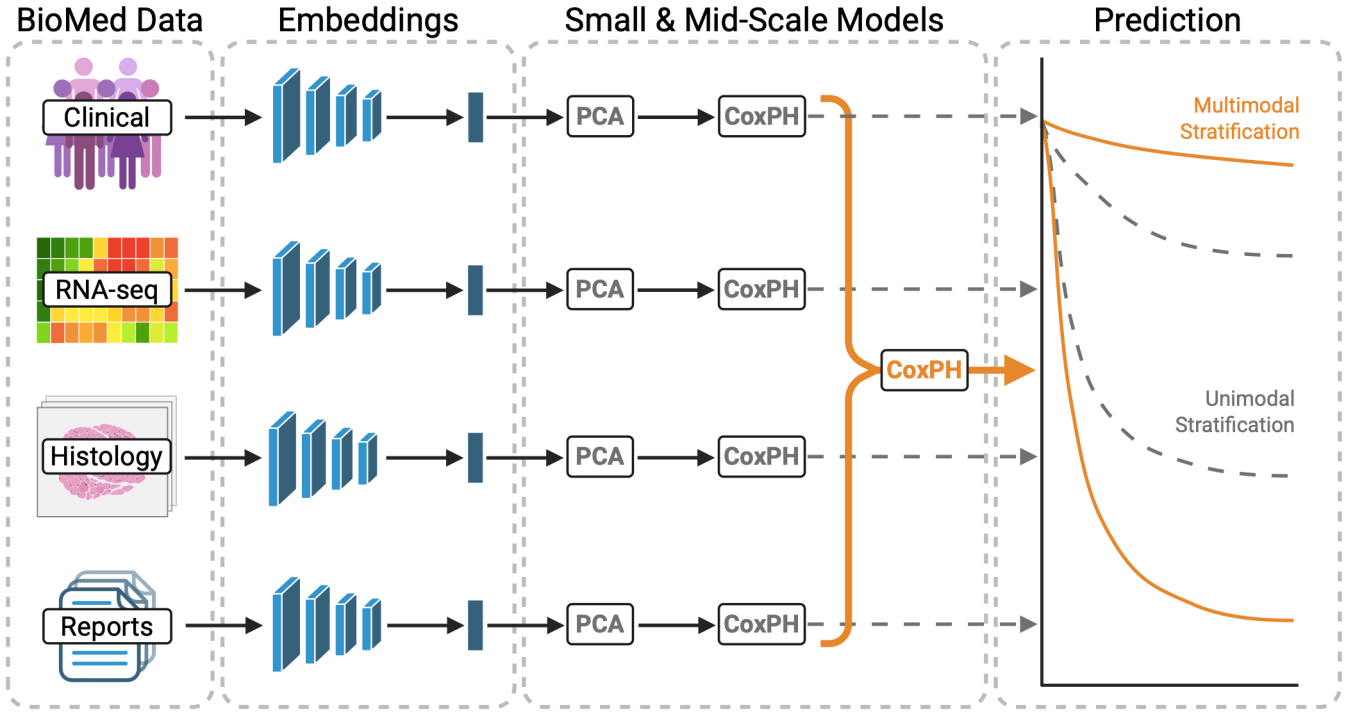


Figure 1: Multimodal survival modeling is vastly simplified in the age of foundation models. Simple ensembles of small, linear models over zero-shot FM embeddings improve pan-cancer survival risk stratification. In our experiments, we further simplify clinical embeddings as one-hot encoded categorical features input directly to CoxPH survival models.

A modern paradigm in biomedical deep learning is the development of foundation models (FMs) to derive meaningful feature embeddings<sup>22</sup>. These FMs are trained over a large corpus of data, typically using a self supervised training objective to improve embedding generalizability to downstream modeling tasks. For example, the Universal Cell Embedding (UCE)<sup>23</sup> model for single-cell RNAseq (scRNAseq) was trained with an adaptation of masked-language modeling (MLM)<sup>24</sup> for gene expression data. Similarly, UNI<sup>25</sup>, an FM for digital pathology, was trained using the DINOv2 framework<sup>26</sup> to produce robust feature embeddings.

Biomedical text especially has seen growing development of large language model (LLM) FMs<sup>27,28</sup>. There have been a series of adaptations of LLMs towards the biomedical domain. The early success of BioMedBERT (formerly PubMedBERT)<sup>29</sup>, a biomedical adaptation of BERT<sup>24</sup>, motivated subsequent works such as BioMedLM (formerly PubMedGPT)<sup>30</sup> and BioMistral<sup>31</sup>, adaptations of GPT-2<sup>32</sup> and Mistral<sup>33</sup>, respectively. While these FMs were trained on text from research articles from PubMed and PubMed Central, more specific pathology-report text FMs have been developed as vision-language models (CONCH<sup>34</sup> and MUSK<sup>35</sup>).

While TCGA contains free-text data as pathology reports, these have been historically underutilized. This may in part be due to both the prior lack of interest in text data compared to the histology or sequencing data and the difficulty of working with the data format of these reports as scanned PDFs. With the current interest in applications of LLMs to biomedical domains, a recent effort used optical character recognition to extract the text from all available PDFs of the TCGA<sup>36</sup>. To the best of our knowledge, only one other work has explored the application of the TCGA reports towards survival modeling<sup>35</sup> and differs from our approach (see Discussion).

Here, we investigate the combination of classical survival models with modern FMs for predicting cancer survival using multimodal data from the TCGA, including pathology report text. Figure 1 presents a visual overview of our proposed framework. Our key findings are:

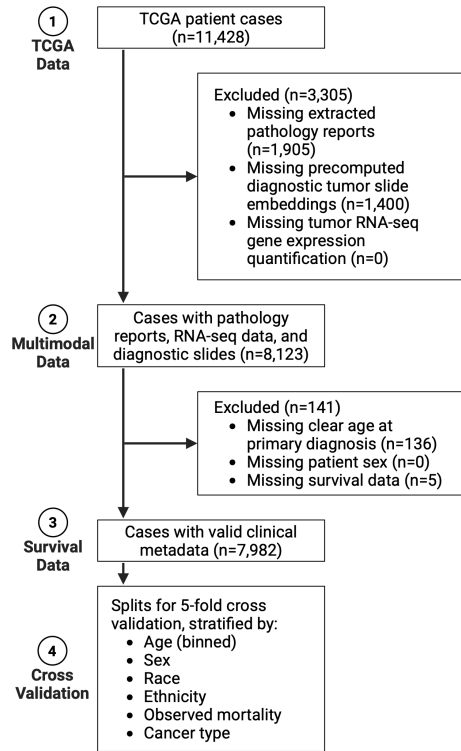


Figure 2: Eight thousand patient cases spanning 32 cancer types with survival data, pathology reports, diagnostic slides, and gene expression.

- **FM-based embeddings can be computed in low resource environments and then used as inputs to statistical or standard machine learning models.** This approach does not require the extensive GPU-based computing resources needed for supervised fine-tuning of large language or foundation models, achieves comparable performance to literature<sup>35</sup>, and does not risk data leakage through fine-tuning.
- **Classical survival models predict survival using FM embeddings.** We fit Cox proportional hazards (CoxPH)<sup>37</sup> models over zero-shot embeddings extracted by FMs reduced with principal component analysis (PCA)<sup>38,39</sup>.
- **Multimodal fusion is additive and improves survival predictions.** We use a simple framework to do late-fusion of unimodal survival predictions and show that multimodal fusion outperforms unimodal models.
- **Pathology report summarization improves survival predictions.** We demonstrate the benefit of summarizing pathology report text for survival prediction and rigorously evaluate the effect of text hallucination.

## RESULTS

### Multimodal survival data across 32 cancers

We assemble a dataset of 7,982 patient cases for our study according to the inclusion flowchart presented in Figure 2. These cases span 32 of the 33 cancer types in the TCGA. We select cases that have available and valid data for survival analysis, preextracted pathology reports by

Modality	PCA Dimension							
	4	8	16	32	64	128	256	N/A
Demo*	-	-	-	-	-	-	-	0.630
Canc*	-	-	-	-	-	-	-	0.737
Expr	0.626	0.650	0.702	0.742	0.749	0.753	0.750	-
Hist	0.596	0.631	0.669	0.714	0.733	0.748	0.754	-
Text	0.565	0.610	0.690	0.725	0.745	0.751	0.752	-

Table 1: Foundation model derived embeddings predict survival. Average cross-validated C-index of CoxPH models trained over unimodal embeddings across varying PCA reductions. Demo = demographics, Canc = cancer type, Expr = BulkRNABert embedded RNA-Seq gene expression, Hist = UNI2 embedded histology, Text = BioMistral embedded pathology reports summarized by Llama-3.1-8B-Instruct. \*Demographics and cancer type features were not reduced with PCA.

Modality	Cancer Type (TCGA Project)							
	BRCA	KIRC	UCEC	THCA	LGG	HNSC	LUSC	LUAD
Demographics	0.637	0.600	0.593	0.885	0.727	0.525	0.542	0.530
RNA-seq	0.573	0.673	0.643	0.619	0.790	0.560	0.579	0.620
Histology	0.648	0.685	0.703	0.749	0.753	0.636	0.598	0.617
Text	0.641	0.698	0.723	0.619	0.716	0.582	0.556	0.645
Multimodal	0.720	0.752	0.758	0.787	0.840	0.650	0.626	0.687

Table 2: Multimodal fusion improves pan-cancer survival prediction. Averaged C-index from 5-fold cross-validation for the top 8 most prevalent cancer types in TCGA. Text model used summarized reports. Multimodal model used fusion of all unimodal modalities. Results reported using PCA to 256 dimensions for all foundation model derived embeddings.

Kefeli and Tatonelli<sup>36</sup>, precomputed tumor diagnostic slide embeddings by Chen et al.<sup>25</sup>, and tumor RNA-seq gene expression quantification.

For our experiments, we split the dataset into 5 cross-validation folds that are shared across all experiments. We stratify the splits by age bin, sex, race, ethnicity, observed mortality, and cancer type. Exact descriptive features of our dataset and splits are provided in Tables 7 and 8. While we stratify by cancer type and observed mortality, we do not stratify by survival duration. On average, overall survival time is comparable across splits, however per-cancer type subsets contained within each split may have too few observed mortalities for survival modeling (see Table 8).

## Unimodal FM embeddings predict survival

We fit small, linear CoxPH survival models over unimodal data and attain a peak mean cross-validated concordance index (C-index)<sup>40</sup> of approximately 0.75 over single modalities (Table 1). For categorical demographic features or cancer type, we do no dimensionality reduction. CoxPH models fit over demographic features or cancer type alone achieve lower C-index (0.630 and 0.737, respectively) as compared to models fit over FM-derived embeddings of other biomedical data modalities.

Specifically, we fit and evaluate survival models over aggregated case-level embeddings for each modality. For FM-derived embeddings (expression, histology, and text), we tested varying

Modality	PCA Dimension						
	4	8	16	32	64	128	256
Expr-Hist	0.638	0.665	0.714	0.753	0.765	0.771	0.774
Expr-Text	0.636	0.671	0.724	0.762	0.774	0.779	0.778
Hist-Text	0.606	0.662	0.705	0.746	0.767	0.777	0.780
Expr-Hist-Text	0.644	0.682	0.727	0.765	0.780	0.786	0.788

Table 3: Late, multimodal fusion of unimodal, FM-based survival models improves survival prediction. For modality combinations with only FM-derived embeddings, average cross-validated C-index of multimodal CoxPH models trained over predicted risk scores from unimodal CoxPH models across varying PCA reductions. Expr = BulkRNABert embedded RNA-Seq gene expression, Hist = UNI2 embedded histology, Text = BioMistral embedded pathology reports summarized by Llama-3.1-8B-Instruct.

Modality	PCA Dimension							
	4	8	16	32	64	128	256	N/A
Canc-Demo*	-	-	-	-	-	-	-	0.747
Hist-Text	0.606	0.662	0.705	0.746	0.767	0.777	0.780	-
Expr-Hist-Text	0.644	0.682	0.727	0.765	0.780	0.786	0.788	-
Demo-Expr-Hist-Text	0.680	0.717	0.748	0.776	0.788	0.794	0.795	-
Canc-Demo-Expr-Hist-Text	0.749	0.752	0.760	0.777	0.788	0.793	0.793	-

Table 4: Mixing survival models of clinical features with FM-based survival models improves survival prediction. For the best combination of each number of modality combinations, average cross-validated C-index of multimodal CoxPH models trained over predicted risk scores from unimodal CoxPH models across varying PCA reductions. Demo = demographics, Canc = cancer type, Expr = BulkRNABert embedded RNA-Seq gene expression, Hist = UNI2 embedded histology, Text = BioMistral embedded pathology reports summarized by Llama-3.1-8B-Instruct. \*Demographics and cancer type features were not reduced with PCA.

PCA sizes for dimensionality reduction. We observe a general trend of increasing C-index with increasing PCA dimensions, which plateaus around PCA to 256 dimensions. Based on this observation, we report further results using PCA transformation of these embeddings to 256 dimensions.

We find that using BulkRNABert<sup>41</sup> embeddings for tumor RNA-seq gene expression quantification, we achieve C-index = 0.750. We further find that survival modeling over UNI2<sup>25</sup> derived embeddings of tumor diagnostic histology slides results in C-index = 0.754. For pathology reports, using BioMistral<sup>31</sup> derived embeddings of pathology reports summarized by Llama-3.1-8B-Instruct<sup>42</sup>, we attain C-index = 0.752.

With the same unimodal survival models, we evaluate their survival prediction performance across individual cancer types (Table 2). As the cancer type modality’s features would not differ for samples of the same cancer type, we do not evaluate per-cancer survival based on cancer type. We not only find that survival modeling performance of unimodal models varies across cancer types, we also observe that no single modality generally outperforms the other modalities. For example, among unimodal models, demographic-based modeling was most predictive of thyroid carcinoma (THCA) survival, demographics C-index = 0.885, while the same was true for text report-based modeling of endometrial carcinoma (UCEC) survival, text C-index = 0.723.

Modality	Cancer Type (TCGA Project)							
	BRCA	KIRC	UCEC	THCA	LGG	HNSC	LUSC	LUAD
Original	0.612	0.645	0.575	0.593	0.630	0.574	0.540	0.593
Summarized	0.641	0.698	0.723	0.619	0.716	0.582	0.556	0.645
Multimodal	0.720	0.752	0.758	0.787	0.840	0.650	0.626	0.687

Table 5: Summarization of pathology reports improves pan-cancer survival prediction. Averaged C-index from 5-fold cross-validation for the top 8 most prevalent cancer types in TCGA. All text embedded using BioMistral. Summarized text generated using Llama-3.1-8B-Instruct. Multimodal model incorporates unimodal summarized text model. Results reported using PCA to 256 dimensions for all foundation model derived embeddings.

## Multimodal fusion improves survival prediction

While unimodal models were able to achieve a peak C-index of approximately 0.75, we find that all multimodal fusion models are able to surpass unimodal results at their corresponding PCA reductions (Tables 3 and 4). We again observe a plateau of survival model performance at PCA = 256 and thus report results using this dimensionality reduction for embeddings. Importantly, each modality is independently modeled at a given PCA dimensionality before the predicted unimodal risk scores are subsequently used as input features to the multimodal fusion model (see Methods for more details).

Using this simple, late multimodal fusion technique, we find that fusion of expression with histology data, expression with report data, and histology with report data result in mean cross-validated C-index = 0.774, 0.778, and 0.780, respectively (Table 3). Fusion of all three of expression, histology, and reports results in the best embedding-based model performance of C-index = 0.788. Survival modeling with these embedding-based modalities are not only additive, but also can be further enhanced with clinical features, such as demographics, achieving our greatest C-index = 0.795 (Table 4).

When examining multimodal model performance subset by cancer type in Table 2, we find that multimodal fusion consistently performs better than any other modality within a given cancer type. This is in contrast to the unimodal models where the best unimodal model differs depending on the cancer. Furthermore, across the 8 most common cancer types in our data, we find that the multimodal model's worst performance (C-index = 0.626 for LUSC) does not cross below a C-index of 0.6, whereas each unimodal model does.

## Pathology report summarization focuses survival information

One of our key findings is that LLM summarization of pathology reports drastically improves survival prediction. Specifically, we prompt Llama-3.1-8B-Instruct without any fine-tuning to summarize pathology reports with a focus on microscopic descriptions, test results, diagnoses, and clinical history. See the Methods section for more details on our summarization method.

Using Llama generated summaries, we embed the summarized reports using BioMistral. As compared with BioMistral embeddings of the original, unsummarized reports, we find that the summarized reports are able to better predict survival (C-index = 0.752 for summarized vs C-index = 0.694 for unsummarized). Using the predicted risk scores, we stratify the study cohort into low and high risk groups and observe that summarized reports result in enhanced risk stratification (Figure 3).

Not only does summarization reduce the token length of the original report, it also corrects

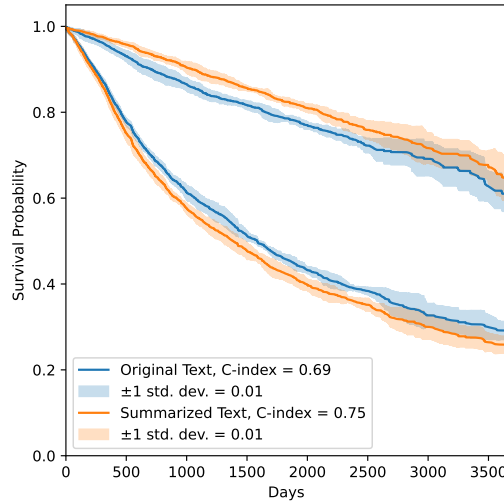


Figure 3: Summarization of pathology reports improves survival model risk stratification over unimodal text embeddings. Embeddings derived with BioMistral. Reports summarized with Llama-3.1-8B-Instruct. Averaged risk stratification from 5-fold cross-validation.

typographical errors that may result from text extraction from the source scanned PDFs of these reports. In addition, prompting the summarization to focus on certain aspects of the report may better extract information most relevant to survival prediction. With these effects in combination, we observe that embeddings of summarization outperforms embeddings of the original report across the 8 most prevalent cancer types (Table 5).

## Hallucination correction does not impact risk stratification

While we empirically find that summarization improves survival prediction, an important consideration with LLM generated text is the effect of hallucinations. To test whether factually incorrect information in the generated summaries impact downstream survival modeling, we perform an experiment whereby we manually correct generated summaries for these hallucinations.

To that end, we develop and share a lightweight tool to facilitate comparison of original and summarized reports. See the Methods section for more details on its usage. This utility runs locally in a web browser and is implemented in pure HTML and JavaScript; it does not require an internet connection to use. A screenshot of the tool is presented in Figure 4.

Using this utility, we review 40 randomly sampled reports contained within a single cross-validation fold. We ultimately apply minor corrections to 24 of 40 reports. The precise methodology for our manual correction process is detailed in our Methods section.

After manual correction, we re-embed the corrected summaries and do survival prediction using the same CoxPH model trained on summarized embeddings. For the subset of corrected reports, we compare against the corresponding uncorrected summaries (Figure 5). We find that risk stratification of the sampled subset does not change based on correction of hallucinations.

## Domain specificity improves survival prediction

Our final set of experiments were ablations to test the impact of foundation model domain specificity for downstream embedding-based survival prediction. For bulk RNA-seq gene expression modality, we compare our default (BulkRNABert) against Universal Cell Embedding (UCE)<sup>23</sup>, a foundation model trained over single cell RNA-seq data. We hypothesized that UCE may still be



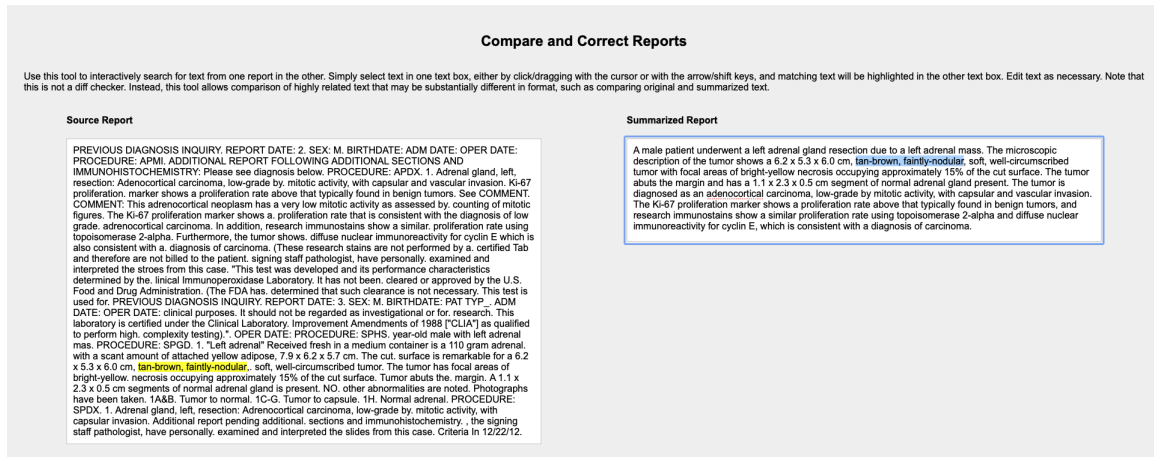


Figure 4: Manual review of generated summaries is facilitated by our simple comparison utility. Users dynamically highlight text between reports and can edit as needed. This is more powerful than traditional diff-checkers as summarized reports often fix typos or contain semantically similar text that is not an exact string match. The tool is implemented in pure HTML/JavaScript and does not require an internet connection to use.

able to extract some meaningful features from the mixture of cellular gene expression profiles present in bulk RNA-seq data. We find that while UCE derived embeddings do contain some prognostic signal (C-index = 0.637, PCA = 256) which stratifies risk (Figure 6), this is significantly lower compared to BulkRNABert derived embeddings (C-index = 0.753, PCA = 256) and even naive cancer type-based survival (C-index = 0.737, Table 1).

Furthermore, given the strong effects of summarization observed in Figure 3, we test the impact of domain specificity for the text embedding. To isolate the effect of domain adaptation, we compare BioMistral derived embeddings against Mistral-7B-Instruct-v0.1 (Mistral)<sup>33</sup> derived embeddings. We compare BioMistral and Mistral embeddings for both original, unsummarized pathology reports and summarized reports (Figure 7).

We find that for unsummarized reports, embedding FM domain adaptation has a small but appreciable effect on 5-fold cross-validated risk stratification, however it does not change survival prediction performance (Mistral C-index = 0.691 vs BioMistral C-index = 0.691, both PCA = 256). For summarized reports, both risk stratification and risk prediction are equivalent (Mistral C-index = 0.751 vs BioMistral C-index = 0.752). Rather, we recapitulate our previous finding that summarization itself has a greater effect for survival modeling. Given their near equivalence and minor improvement in unsummarized report-based risk stratification, we use BioMistral as our default text embedding model.

## DISCUSSION

Our study demonstrates the ease with which multimodal survival modeling is accomplished in the age of foundation models. We show that zero-shot embeddings of unseen data can serve as the basis for prediction of cancer prognosis. We emphasize that our final survival models are combinations of classical Cox proportional hazards models with FM derived embeddings and five tabular, clinical features. The synergy between feature-rich embeddings and simple linear models enables prediction of complex biological tasks<sup>43</sup>. This powerful paradigm in modern deep learning is additionally beneficial in medical settings where data privacy is a chief concern and model tuning can lead to memorization of small datasets of protected patient data<sup>22,44–47</sup>. In our results, though we use open-access TCGA data, we rely on FMs trained over deidentified



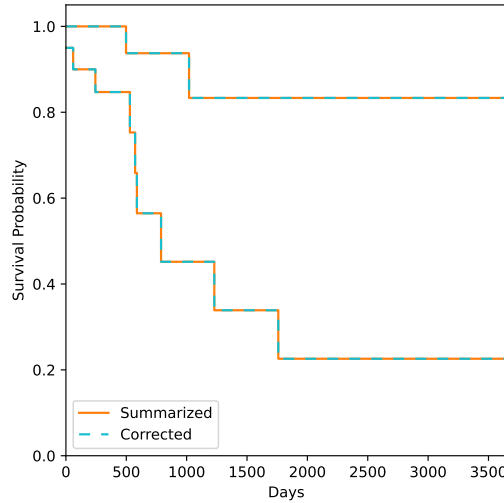


Figure 5: Manual correction of summarized pathology report hallucinations does not impact survival model risk stratification. Embeddings derived with BioMistral. Reports summarized with Llama-3.1-8B-Instruct. Risk stratification from N=40 randomly sampled cases contained within a single test split while preserving observed mortality prevalence.

and often public data. We do not train any deep learning models. It is important to note that this approach applies to low resource environments that do not have the computing infrastructure for supervised fine tuning of deep, large language, or foundation models.

Importantly, we compare survival models over more complex modalities against survival models over basic clinical tabular features spanning four demographic features (age, sex, race, ethnicity) and cancer type. While our unimodal survival predictions over embeddings of expression, histology, or text data are better than demographic features alone, they are comparable to cancer type alone and equivalent to the fusion of demographic and cancer type predictions. Indeed, survival rates vary by cancer type as a complex interaction of biological and socioeconomic factors<sup>48</sup>, however survival prediction within a given cancer cannot be predicted by the cancer type itself. Thus, our unimodal models over foundational embeddings still demonstrate predictive power, especially when examining prognoses within cancer types.

The results from our simple framework for multimodal survival modeling additionally show that learned information from single modalities is additive and that multimodal fusion is able to achieve impressive prediction accuracy. This additive effect may be explained by the varying unimodal results for per-cancer survival modeling. We find that no single unimodal model excels across all of eight of the most prevalent cancer types in TCGA. Further, each unimodal model (of demographics, expression, histology, and text modalities) does best for a specific cancer type. Contrary to other work, we find that information extracted by FMs for these modalities can be overall additive<sup>49</sup>, even if they may be redundant in some cases.

Compared to other works investigating multimodal survival models<sup>13–21,49</sup>, we propose a simple yet effective late fusion strategy. We use the predicted risk scores of unimodal models as input to the final multimodal CoxPH model. This further modularizes the modeling of individual modalities (in addition to FM embeddings) and allows the multimodal model to be agnostic to unimodal embeddings. This abstraction simplifies challenges of other fusion approaches. For example, ensuring smaller dimensionality features (such as demographics) are modeled comparably to higher dimensional features (such as expression embeddings) is accomplished implicitly in our framework. Given this, we experiment with varying embedding methods for our high-dimensional feature modalities.

We specifically experiment with alternate embeddings for expression and text data. First, for

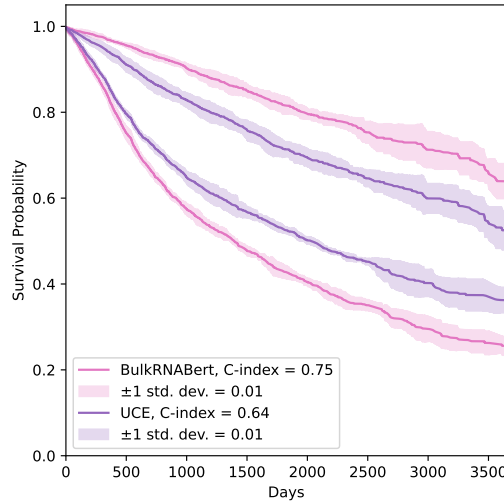


Figure 6: Modality specificity of gene expression embedding model improves survival model risk stratification over unimodal gene expression embeddings. Bulk RNA-seq data embedded with either BulkRNABert or UCE, a single-cell RNA-seq model. Averaged risk stratification from 5-fold cross-validation.

expression data, we hypothesized that a single-cell RNA-seq (scRNA-seq) FM may generalize to the mixed cellular identities of bulk RNA-seq data. While many scRNA-seq FMs exist<sup>50</sup>, we chose UCE specifically based on its reported strong performance at extracting multiscale embeddings of cellular biology<sup>23</sup>. We find that while UCE derived embeddings of bulk RNA-seq data does contain prognostic information, it is comparable to demographic-based survival prediction. Perhaps unsurprisingly, survival prediction based on UCE embeddings is far surpassed by modality-specific embeddings by BulkRNABert.

For the pathology report text modality, we choose BioMistral for its long context length and general biomedical domain adaptation, as opposed to other long-context LLMs adapted to more specific clinical domains<sup>51</sup> unrelated to pathology reports. More specific pathology language models such as CONCH<sup>34</sup> or MUSK<sup>35</sup> have been reported, however they are limited by extremely short contexts of 128 and 100 tokens, respectively. In our data, using the Mistral tokenizer (shared by BioMistral), the longest report is 8,184 tokens and the longest summarized report is 1,389 tokens. Despite BioMistral’s domain adaptation with a context length of 2,048, the base Mistral model’s context length of 8,196 and its sliding window attention<sup>52</sup> enable a theoretical maximum context length that fits all of our pathology reports without truncation. Future work is needed to explore LLMs domain adapted at the full context length.

To the best of our knowledge, Xiang et al.<sup>35</sup> are the only other group to have explored multimodal survival modeling with pathology reports. While they also utilize summarization of text reports to condense their pathology reports, our work differs in key ways. First, unlike the MUSK authors, we do training of our foundation models and evaluate zero-shot extracted embeddings. Yet their reported multimodal C-index of 0.747 is comparable to our unimodal results, including naive cancer-type based prediction. Our multimodal fusion of histology and text resulted in C-index = 0.780. We additionally incorporate gene expression and clinical data, alongside histology and text modalities, achieving C-index = 0.795 and further surpassing their dual modality results. Experimentally, due to their language model length limitation, they cannot compare to unsummarized reports as we have. Lastly, their text summarization differs per cancer type, requiring specific, hand-written prompts by an oncologist; while this may focus the most relevant information for a given cancer type, it is not as generalizable to other cancer types as our broad summarization prompt.

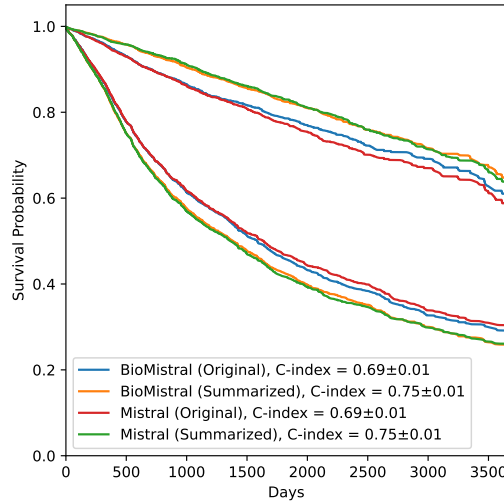


Figure 7: Domain adaptation of text embedding model improves survival model risk stratification over unimodal text embeddings. Embeddings derived with either BioMistral or Mistral-7B-Instruct-v0.1. Reports summarized with Llama-3.1-8B-Instruct. Averaged risk stratification from 5-fold cross-validation.

We find that our general summarization strategy greatly improves survival prediction using the text modality. Using these generated summaries, we evaluate the effect of hallucinations in model generated summaries. To that end, we develop, utilize, and share an interactive tool to greatly facilitate the process of manually reviewing and correcting generated summaries. For a subset of 40 randomly sampled summarized reports, we find the need to correct 24 of the generated summaries. Qualitatively, many of these corrections involved small details relative to the rest of the summary, for example correcting the number of lymph nodes negative for metastases. We found manual correction did not change the risk stratification of the sampled subpopulation compared to uncorrected summaries. While this was true in our study, we emphasize the importance of this kind of experiment, especially as researchers and users increasingly rely on model generated text.

Overall, our study presents a lightweight framework for multimodal survival modeling leveraging foundation model derived embeddings with classical models. We demonstrate that embeddings of expression, histology, and text data each independently predict survival. Additionally, we show that these modalities are additive using a simple late fusion technique, leaving the door open for expansion to additional modalities. We present novel results on pathology report-based survival prediction and the effects of LLM hallucinations in summarizing those reports for survival tasks. Altogether, these findings represent an important opportunity for the application and evaluation of FMs towards potential resource and data limited settings and settings necessitating protection of data privacy, such as prediction of patient survival using multiomic data.

## METHODS

All code for our experiments are available on GitHub at: <https://github.com/StevenSong/multimodal-cancer-survival>. These methods are the culmination of initial experimentation and hyperparameter search implemented across separate code bases, linked from our standalone repository for this work.

Line	Role	Message
1	System	You are a helpful assistant for digital pathology.
2	System	Instructions: Extract and repeat the results of the following pathology report in a single paragraph. Focus on test results, diagnoses and clinical history. Include results of the microscopic description. Omit the gross or macroscopic description. Do not acknowledge this prompt. Do not give additional comments after your final answer.
3	User	(Pathology Report)

Table 6: Pathology report summarization prompt.

## Data and Experimental Setup

We use TCGA patient cases which have available and valid survival data, pathology reports, tumor diagnostic slides, and tumor RNA-seq gene expression. For pathology reports, we use text extracted by Kefeli and Tatonetti<sup>36</sup>. For computational efficiency, we additionally rely on precomputed UNI2 embeddings of diagnostic slides by Chen et al.<sup>25</sup>. Given these requirements, we first filter TCGA cases by the availability of pathology report, diagnostic slide, then RNA-seq data. We download the extracted text from Mendeley<sup>53</sup>, precomputed UNI2 embeddings of diagnostic slides from HuggingFace<sup>54</sup>, and RNA-seq data using the Genomic Data Commons (GDC) API<sup>2</sup>. We ensure that the RNA-seq and diagnostic slides are derived from tumor samples.

We then select cases with valid demographic and survival data, again downloaded using the GDC API. Specifically, we compute survival as the time between the patient’s age at primary diagnosis and the patient’s age at last followup or death. We additionally require non-missing patient sex. Given the final set of cases, we split our dataset for 5-fold cross-validation. We stratify by patient age, sex, race, ethnicity, mortality, and cancer type. To stratify by age, we discretize age into 20-year age bins, i.e. [0-20), [20-40), [40-60), [60-80), and 80+. For race and ethnicity, missing values are replaced with “Not Reported”. We one-hot encode demographic features (binned age, sex, race, ethnicity) and cancer type (TCGA project) for stratification and downstream modeling, resulting in 17 and 32 features, respectively.

## Report Summarization

While the extracted pathology reports<sup>36</sup> are a rich source of information, they present multiple challenges. As the source reports are scanned documents of varying quality, the OCR extraction process can result in typos and loss of structured text. Additionally, the reports are often long with repeated information or information potentially irrelevant for cancer prognosis (e.g. incidental findings on histology).

To address these challenges, we experiment with having an LLM summarize the pathology reports to help focus relevant information, correct typos, and reduce report length. We choose Llama-3.1-8B-Instruct as the summarization model for its strong instruction following capabilities. We use vLLM<sup>55</sup> for inference with set seed, greedy decoding, temperature 0, and max tokens 1,024. The precise prompt we use is presented in Table 6.

## Foundation Model Embeddings

We use several foundation models in our experiments. For all FMs, we use the models as-is with no further training or fine-tuning. We ensure that the FMs we use have not been trained over TCGA to prevent data leakage.

For diagnostic slides, we use UNI2-h<sup>25</sup> precomputed embeddings. Notably, as UNI2 is a tile/patch-level encoder, we aggregate tile embeddings to a slide-level embedding using simple averaging. Each UNI2 embedding is 1536 dimensional.

For pathology reports or their summaries, we embed text using BioMistral-7B<sup>31</sup> or its source model, Mistral-7B-Instruct-v0.1<sup>33</sup>. We perform embedding inference for these LLMs using vLLM<sup>55</sup>. Each BioMistral or Mistral embeddings is 4096 dimensional.

For gene expression data, we experiment with both BulkRNABert<sup>41</sup> and Universal Cell Embedding (UCE)<sup>23</sup>. For BulkRNABert, to prevent data leakage, we specifically use the model checkpoint trained over GTEx<sup>56</sup> and ENCODE<sup>57</sup> data. For UCE, we use the 33-layer model variant trained over data from CELLxGENE<sup>58</sup>. We make minor modifications to the code repositories for both of these models to enable installation as pip packages and inline data processing. The forks of these repositories containing our modifications are linked from our main GitHub repo. BulkRNABert embeddings are 256 dimensional and UCE embeddings are 1280 dimensional.

As survival is defined at the patient-level, we aggregate patient embeddings from multiple samples of the same modality into a single embedding per patient per modality. This is most relevant for RNA-seq and diagnostic slides as a patient may have multiple samples for these modalities. We use simple averaging of embeddings to derive our patient-level embeddings.

## Unimodal and Multimodal Survival Modeling

Given patient-level, modality-specific embeddings, we adopt a simple pipeline for unimodal survival modeling. For a given train-test split, we z-score standardize all embeddings using per-feature mean and standard deviation derived from the training split. We next derive a PCA dimensionality reduction over the standardized embeddings from the training split and apply to all standardized embeddings. We use the implementation of PCA from sklearn<sup>59</sup> with a set seed. We experiment with varying PCA dimensions, doubling from 4 to 256. For demographic or cancer type modalities, features are one-hot encoded so we do not apply standardization or PCA transformation. We then fit a Cox proportional hazards (CoxPH)<sup>37</sup> to the PCA reduced embeddings (or the one-hot encoded features for demographic or cancer type modalities) of the train split. We use the implementation of CoxPH models from sksurv<sup>60</sup> with  $\alpha = 0.1$  for ridge regression penalty. Using the trained model, we predict risk scores for both the train and test splits for further modeling and evaluation. We repeat this unimodal procedure for all data modalities.

We do late multimodal fusion using the predicted unimodal risk scores as input to the multimodal model. Given a set of modalities we aim to fuse, we concatenate the predicted risk scores from each modality as input features. We z-score standardize each feature using the mean and standard deviation derived over the training split. We fit a CoxPH model over the concatenated, standardized, unimodal risk scores. Using the trained multimodal model, we predict risk scores for the test split for evaluation. We repeat this multimodal fusion procedure over all combinations of demographic, cancer type, histology, expression, and text modalities. Notably, we do not consider alternate embedding methods as separate modalities; for example BioMistral embeddings of unsummarized and summarized reports are both text embeddings. Instead, we consider multimodal combinations with these alternate embedding strategies independently.

## Evaluation of Survival Models

Our primary evaluation metric for our survival models is the concordance index (C-index)<sup>40</sup>. For each model, we report the average C-index derived over the test split from 5 cross-validation folds. For model performance by cancer type, we compute the C-index over only cases belonging to each cancer type; as our cross-validation folds are stratified by cancer type and mortality, the number of cases and observed deaths for a given cancer type across folds is equivalent.

To visualize the prognostic capability of our models, we plot averaged risk stratification curves. For a given test split, we binarize the predicted risk about the median into high and low risk groups. For both the low and high risk groups, we compute their Kaplan-Meier curves<sup>61</sup>. We repeat this procedure for each cross-validation fold. To compute the average survival curve, we first impute the curves to a shared set of time points before averaging across folds. When visually appropriate, we include shaded regions about the average curves denoting one standard deviation at each time point.

The only exception to our cross-validated evaluation is in our experiment to manually correct hallucinations in model generated summaries, further described below.

## Manual Correction of Summaries

As we experiment with Llama-3.1 generated summaries of pathology reports, we test the effect of model hallucinations in the generated summaries and their downstream effects on survival modeling. To that end, we manually review model generated summaries for 40 randomly selected cases contained within a single test split. We randomly select these cases while preserving the overall prevalence of observed mortality. After review and manual correction (as needed) of the sampled summaries, we embed the corrected summaries using BioMistral and apply the CoxPH model trained over BioMistral embeddings of summaries from the corresponding train split. We evaluate risk stratification over these sampled cases. As these cases are contained within a single cross-validation fold, we do not report aggregate evaluations for this experiment.

In our manual correction of generated summaries, we only change factually incorrect information based on information from the original report. We do not add extra information that was not already present in the summary. When the incorrect information cannot be corrected based on the original report, we delete the erroneous text. A salient example of this was when patient age was redacted in the original report. The resulting extracted text thus contained a fragment such as “-year-old patient”, which the summarizing LLM interpreted to mean a 1-year-old patient. Manual verification of the case metadata revealed the patient to be in their 40s, however, because this data was impossible to derive from the original report, we remove the mention of the patient age in the corrected summary. All manual corrections for our experiment were done by a medical student who had completed two years of preclinical medical education.

For manual correction of summaries, we develop and share a lightweight, interactive tool for comparing unsummarized and summarized reports. The tool allows users to select sections of text in one text box which are automatically highlighted in the other text box. This enables users to quickly and interactively find corresponding information in large spans of text, thus facilitating verification of summaries using the source report. The tool is implemented in pure HTML and JavaScript and runs locally in a web browser, requiring no internet connection to use. We share the tool and a demo video of its use in our GitHub repository.

## RESOURCE AVAILABILITY

### Lead contact

Requests for further information and resources should be directed to and will be fulfilled by the lead contact, Robert L. Grossman (rgrossman1@uchicago.edu).

### Materials availability

Our interactive report comparison tool that was created as part of this study is available through our GitHub repository: <https://github.com/StevenSong/multimodal-cancer-survival>.

### Data and code availability

- Source code for all experiments are available in our GitHub repository: <https://github.com/StevenSong/multimodal-cancer-survival>.
- All data are derived from TCGA and are available for public use. Extracted pathology reports are available from Mendely under the DOI 10.17632/hyg5xkznp.1. Precomputed UNI2 embeddings of tumor diagnostic slides are available from HuggingFace datasets under the identifier MahmoodLab/UNI2-h-features. All other data are available through the GDC API.
- Model weights for BioMistral, Mistral-7B-Instruct-v0.1, Llama-3.1-8B-Instruct, UNI2 are available from HuggingFace. Model weights for BulkRNABert and UCE are available from the author's respective code repositories.
- Any additional information required to reanalyze the data reported in this paper is available from the lead contact upon request.

## ACKNOWLEDGMENTS

S.S. is supported by training grant T32GM007281.

## AUTHOR CONTRIBUTIONS

Conceptualization, S.S., M.B.W., and I.M.; methodology, S.S. and M.B.W.; data preparation, S.S. and I.M.; implementation, S.S. and M.B.W.; writing, review & editing, S.S., R.L.G, M.B.W., and I.M.; supervision, R.L.G.

## DECLARATION OF INTERESTS

I.M. is a consultant for VantAI.



## SUPPLEMENTAL INFORMATION INDEX

Table 7. Dataset characteristics for patient demographics and outcomes.

Table 8. Dataset characteristics for cancer types.

	Overall	Cross-Validation Fold			
		0	1	2	3
n	7982	1597	1597	1596	1596
Age, mean (SD)	59.8 (14.4)	59.7 (14.4)	59.9 (14.2)	59.9 (14.5)	59.9 (14.3)
Sex, n (%)	Female	828 (51.8)	842 (52.7)	845 (52.9)	836 (52.4)
	Male	769 (48.2)	755 (47.3)	751 (47.1)	760 (47.6)
Race, n (%)	White	1212 (75.4)	1203 (75.3)	1207 (75.6)	1203 (75.4)
	Black or AA	154 (9.6)	152 (9.5)	165 (10.3)	160 (10.0)
	Asian	72 (4.5)	78 (4.9)	77 (4.8)	78 (4.9)
	AIAN	3 (0.2)	6 (0.4)	2 (0.1)	3 (0.2)
	NHPI	3 (0.2)	2 (0.1)	1 (0.1)	1 (0.1)
	Unknown	24 (1.5)	28 (1.8)	24 (1.5)	21 (1.3)
	Not Reported	638 (8.0)	129 (8.1)	120 (7.5)	130 (8.1)
					131 (8.2)
Ethnicity, n (%)	Not Hispanic/Latino	1197 (75.0)	1197 (75.0)	1197 (75.0)	1192 (74.7)
	Hispanic/Latino	62 (3.9)	56 (3.5)	59 (3.7)	68 (4.3)
	Unknown	37 (2.3)	39 (2.4)	40 (2.5)	31 (1.9)
	Not Reported	1518 (19.0)	301 (18.8)	300 (18.8)	305 (19.1)
Mortality, n (%)	Alive	5790 (72.5)	1166 (73.0)	1152 (72.0)	1165 (73.0)
	Dead	2192 (27.5)	431 (27.0)	444 (27.8)	431 (27.0)
Survival Time in Days, mean (SD)	1026.6 (964.2)	1048.0 (978.4)	1029.3 (969.7)	1013.8 (956.0)	1021.0 (961.9)
					1020.8 (955.5)

Table 7: Survival prediction using eight thousand patient cases spanning 32 cancer types from the TCGA. All cases have clinical, RNA-seq gene expression, diagnostic histology slides, and pathology reports. Patients split for 5-fold cross-validation, stratified by age bins, sex, race, ethnicity, observed mortality, and cancer type. AA = African American, AIAN = American Indian or Alaska Native, NHPI = Native Hawaiian or Pacific Islander.

		Cross-Validation Fold					
		Overall	0	1	2	3	4
Cancer Type, n (%)	n	7982	1597	1597	1596	1596	1596
	ACC	53 (0.7)	11 (0.7)	9 (0.6)	11 (0.7)	11 (0.7)	11 (0.7)
	BLCA	343 (4.3)	67 (4.2)	69 (4.3)	71 (4.4)	67 (4.2)	69 (4.3)
	BRCA	982 (12.3)	197 (12.3)	194 (12.1)	197 (12.3)	198 (12.4)	196 (12.3)
	CESC	248 (3.1)	49 (3.1)	47 (2.9)	50 (3.1)	50 (3.1)	52 (3.3)
	CHOL	33 (0.4)	8 (0.5)	6 (0.4)	5 (0.3)	6 (0.4)	8 (0.5)
	COAD	391 (4.9)	78 (4.9)	77 (4.8)	77 (4.8)	81 (5.1)	78 (4.9)
	DLBC	43 (0.5)	9 (0.6)	9 (0.6)	8 (0.5)	9 (0.6)	8 (0.5)
	ESCA	116 (1.5)	23 (1.4)	26 (1.6)	23 (1.4)	23 (1.4)	21 (1.3)
	GBM	142 (1.8)	29 (1.8)	29 (1.8)	28 (1.8)	28 (1.8)	28 (1.8)
	HNSC	433 (5.4)	89 (5.6)	88 (5.5)	87 (5.5)	83 (5.2)	86 (5.4)
	KICH	65 (0.8)	13 (0.8)	13 (0.8)	13 (0.8)	13 (0.8)	13 (0.8)
	KIRC	497 (6.2)	97 (6.1)	100 (6.3)	102 (6.4)	99 (6.2)	99 (6.2)
	KIRP	237 (3.0)	48 (3.0)	48 (3.0)	46 (2.9)	48 (3.0)	47 (2.9)
	LGG	442 (5.5)	88 (5.5)	90 (5.6)	89 (5.6)	86 (5.4)	89 (5.6)
	LIHC	319 (4.0)	62 (3.9)	63 (3.9)	63 (3.9)	67 (4.2)	64 (4.0)
	LUAD	411 (5.1)	84 (5.3)	83 (5.2)	82 (5.1)	80 (5.0)	82 (5.1)
	LUSC	418 (5.2)	82 (5.1)	82 (5.1)	85 (5.3)	85 (5.3)	84 (5.3)
	MESO	66 (0.8)	15 (0.9)	13 (0.8)	12 (0.8)	12 (0.8)	14 (0.9)
	OV	42 (0.5)	7 (0.4)	10 (0.6)	9 (0.6)	7 (0.4)	9 (0.6)
	PAAD	168 (2.1)	34 (2.1)	32 (2.0)	34 (2.1)	34 (2.1)	34 (2.1)
	PCPG	171 (2.1)	34 (2.1)	37 (2.3)	34 (2.1)	34 (2.1)	32 (2.0)
	PRAD	326 (4.1)	67 (4.2)	66 (4.1)	66 (4.1)	63 (3.9)	64 (4.0)
	READ	144 (1.8)	29 (1.8)	28 (1.8)	29 (1.8)	30 (1.9)	28 (1.8)
	SARC	240 (3.0)	49 (3.1)	50 (3.1)	47 (2.9)	47 (2.9)	47 (2.9)
	SKCM	94 (1.2)	19 (1.2)	19 (1.2)	17 (1.1)	19 (1.2)	20 (1.3)
	STAD	269 (3.4)	52 (3.3)	54 (3.4)	55 (3.4)	54 (3.4)	54 (3.4)
	TGCT	87 (1.1)	19 (1.2)	16 (1.0)	15 (0.9)	18 (1.1)	19 (1.2)
	THCA	483 (6.1)	96 (6.0)	96 (6.0)	97 (6.1)	98 (6.1)	96 (6.0)
	THYM	109 (1.4)	20 (1.3)	21 (1.3)	23 (1.4)	24 (1.5)	21 (1.3)
	UCEC	494 (6.2)	99 (6.2)	100 (6.3)	97 (6.1)	99 (6.2)	99 (6.2)
	UCS	52 (0.7)	11 (0.7)	10 (0.6)	10 (0.6)	10 (0.6)	11 (0.7)
	UVM	64 (0.8)	12 (0.8)	12 (0.8)	14 (0.9)	13 (0.8)	13 (0.8)

Table 8: Eight thousand patient cases span 32 cancer types from the TCGA. Cancer types stratified across 5-fold cross-validation splits.

## References

1. Tomczak, K., Czerwińska, P., and Wiznerowicz, M. (2015). Review the cancer genome atlas (tcga): an immeasurable source of knowledge. *Contemporary Oncology/Współczesna Onkologia* 2015, 68–77.
2. Heath, A.P., Ferretti, V., Agrawal, S., An, M., Angelakos, J.C., Arya, R., Bajari, R., Baqar, B., Barnowski, J.H., Burt, J. et al. (2021). The nci genomic data commons. *Nature genetics* 53, 257–262.
3. Zhang, Z., Hernandez, K., Savage, J., Li, S., Miller, D., Agrawal, S., Ortuno, F., Staudt, L.M., Heath, A., and Grossman, R.L. (2021). Uniform genomic data analysis in the nci genomic data commons. *Nature communications* 12, 1226.
4. Abbasi, A.F., Asim, M.N., Ahmed, S., Vollmer, S., and Dengel, A. (2024). Survival prediction landscape: an in-depth systematic literature review on activities, methods, tools, diseases, and databases. *Frontiers in Artificial Intelligence* 7, 1428501.
5. Arjmand, B., Hamidpour, S.K., Tayanloo-Beik, A., Goodarzi, P., Aghayan, H.R., Adibi, H., and Larijani, B. (2022). Machine learning: a new prospect in multi-omics data analysis of cancer. *Frontiers in Genetics* 13, 824451.
6. Liu, J., Lichtenberg, T., Hoadley, K.A., Poisson, L.M., Lazar, A.J., Cherniack, A.D., Kovatich, A.J., Benz, C.C., Levine, D.A., Lee, A.V. et al. (2018). An integrated tcga pan-cancer clinical data resource to drive high-quality survival outcome analytics. *Cell* 173, 400–416.
7. Wulczyn, E., Steiner, D.F., Xu, Z., Sadhwani, A., Wang, H., Flament-Auvigne, I., Mermel, C.H., Chen, P.H.C., Liu, Y., and Stumpe, M.C. (2020). Deep learning-based survival prediction for multiple cancer types using histopathology images. *PloS one* 15, e0233678.
8. Yang, Z., Wei, T., Liang, Y., Yuan, X., Gao, R., Xia, Y., Zhou, J., Zhang, Y., and Yu, Z. (2025). A foundation model for generalizable cancer diagnosis and survival prediction from histopathological images. *Nature Communications* 16, 2366.
9. Ching, T., Zhu, X., and Garmire, L.X. (2018). Cox-nnet: an artificial neural network method for prognosis prediction of high-throughput omics data. *PLoS computational biology* 14, e1006076.
10. Huang, Z., Johnson, T.S., Han, Z., Helm, B., Cao, S., Zhang, C., Salama, P., Rizkalla, M., Yu, C.Y., Cheng, J. et al. (2020). Deep learning-based cancer survival prognosis from rna-seq data: approaches and evaluations. *BMC medical genomics* 13, 1–12.
11. Qiu, Y.L., Zheng, H., Devos, A., Selby, H., and Gevaert, O. (2020). A meta-learning approach for genomic survival analysis. *Nature communications* 11, 6350.
12. Nayshool, O., Kol, N., Javaski, E., Amariglio, N., and Rechavi, G. (2022). Surviveai: Long term survival prediction of cancer patients based on somatic rna-seq expression. *Cancer Informatics* 21, 11769351221127875.
13. Chaudhary, K., Poirion, O.B., Lu, L., and Garmire, L.X. (2018). Deep learning-based multi-omics integration robustly predicts survival in liver cancer. *Clinical cancer research* 24, 1248–1259.

14. Zhan, X., Cheng, J., Huang, Z., Han, Z., Helm, B., Liu, X., Zhang, J., Wang, T.F., Ni, D., and Huang, K. (2019). Correlation analysis of histopathology and proteogenomics data for breast cancer. *Molecular & Cellular Proteomics* 18, S37–S51.
15. Hao, J., Kim, Y., Mallavarapu, T., Oh, J.H., and Kang, M. (2019). Interpretable deep neural network for cancer survival analysis by integrating genomic and clinical data. *BMC medical genomics* 12, 1–13.
16. Ramirez, R., Chiu, Y.C., Zhang, S., Ramirez, J., Chen, Y., Huang, Y., and Jin, Y.F. (2021). Prediction and interpretation of cancer survival using graph convolution neural networks. *Methods* 192, 120–130.
17. Malik, V., Kalakoti, Y., and Sundar, D. (2021). Deep learning assisted multi-omics integration for survival and drug-response prediction in breast cancer. *BMC genomics* 22, 1–11.
18. Redekar, S.S., Varma, S.L., and Bhattacharjee, A. (2022). Identification of key genes associated with survival of glioblastoma multiforme using integrated analysis of tcga datasets. *Computer Methods and Programs in Biomedicine Update* 2, 100051.
19. Sun, B., and Chen, L. (2023). Interpretable deep learning for improving cancer patient survival based on personal transcriptomes. *Scientific Reports* 13, 11344.
20. Fan, Z., Jiang, Z., Liang, H., and Han, C. (2023). Pancancer survival prediction using a deep learning architecture with multimodal representation and integration. *Bioinformatics Advances* 3, vbad006.
21. Hao, Y., Jing, X.Y., and Sun, Q. (2023). Cancer survival prediction by learning comprehensive deep feature representation for multiple types of genetic data. *BMC bioinformatics* 24, 267.
22. Bommasani, R., Hudson, D.A., Adeli, E., Altman, R., Arora, S., von Arx, S., Bernstein, M.S., Bohg, J., Bosselut, A., Brunskill, E. et al. (2021). On the opportunities and risks of foundation models. *arXiv preprint arXiv:2108.07258*.
23. Rosen, Y., Roohani, Y., Agarwal, A., Samotorčan, L., Consortium, T.S., Quake, S.R., and Leskovec, J. (2023). Universal cell embeddings: A foundation model for cell biology. *bioRxiv* pp. 2023–11.
24. Devlin, J., Chang, M.W., Lee, K., and Toutanova, K. (2019). Bert: Pre-training of deep bidirectional transformers for language understanding. In *Proceedings of the 2019 conference of the North American chapter of the association for computational linguistics: human language technologies, volume 1 (long and short papers)*. pp. 4171–4186.
25. Chen, R.J., Ding, T., Lu, M.Y., Williamson, D.F., Jaume, G., Song, A.H., Chen, B., Zhang, A., Shao, D., Shaban, M. et al. (2024). Towards a general-purpose foundation model for computational pathology. *Nature Medicine* 30, 850–862.
26. Oquab, M., Darcet, T., Moutakanni, T., Vo, H., Szafraniec, M., Khalidov, V., Fernandez, P., Haziza, D., Massa, F., El-Nouby, A. et al. (2023). Dinov2: Learning robust visual features without supervision. *arXiv preprint arXiv:2304.07193*.
27. Singhal, K., Azizi, S., Tu, T., Mahdavi, S.S., Wei, J., Chung, H.W., Scales, N., Tanwani, A., Cole-Lewis, H., Pfohl, S. et al. (2023). Large language models encode clinical knowledge. *Nature* 620, 172–180.

28. Thirunavukarasu, A.J., Ting, D.S.J., Elangovan, K., Gutierrez, L., Tan, T.F., and Ting, D.S.W. (2023). Large language models in medicine. *Nature medicine* 29, 1930–1940.
29. Gu, Y., Tinn, R., Cheng, H., Lucas, M., Usuyama, N., Liu, X., Naumann, T., Gao, J., and Poon, H. (2021). Domain-specific language model pretraining for biomedical natural language processing. *ACM Transactions on Computing for Healthcare (HEALTH)* 3, 1–23.
30. Bolton, E., Venigalla, A., Yasunaga, M., Hall, D., Xiong, B., Lee, T., Daneshjou, R., Frankle, J., Liang, P., Carbin, M. et al. (2024). Biomedlm: A 2.7 b parameter language model trained on biomedical text. *arXiv preprint arXiv:2403.18421*.
31. Labrak, Y., Bazoge, A., Morin, E., Gourraud, P.A., Rouvier, M., and Dufour, R. (2024). Biomistral: A collection of open-source pretrained large language models for medical domains. *arXiv preprint arXiv:2402.10373*.
32. Radford, A., Wu, J., Child, R., Luan, D., Amodei, D., Sutskever, I. et al. (2019). Language models are unsupervised multitask learners. *OpenAI blog* 1, 9.
33. Jiang, A.Q., Sablayrolles, A., Mensch, A., Bamford, C., Chaplot, D.S., de Las Casas, D., Bressand, F., Lengyel, G., Lample, G., Saulnier, L., Lavaud, L.R., Lachaux, M.A., Stock, P., Scao, T.L., Lavril, T., Wang, T., Lacroix, T., and Sayed, W.E. (2023). Mistral 7b. *arXiv preprint arXiv:2310.06825*.
34. Lu, M.Y., Chen, B., Williamson, D.F., Chen, R.J., Liang, I., Ding, T., Jaume, G., Odintsov, I., Le, L.P., Gerber, G. et al. (2024). A visual-language foundation model for computational pathology. *Nature Medicine* 30, 863–874.
35. Xiang, J., Wang, X., Zhang, X., Xi, Y., Eweje, F., Chen, Y., Li, Y., Bergstrom, C., Gopaulchan, M., Kim, T. et al. (2025). A vision–language foundation model for precision oncology. *Nature* pp. 1–10.
36. Kefeli, J., and Tatonetti, N. (2024). Tcga-reports: A machine-readable pathology report resource for benchmarking text-based ai models. *Patterns* 5.
37. Cox, D.R. (1972). Regression models and life-tables. *Journal of the Royal Statistical Society: Series B (Methodological)* 34, 187–202.
38. Pearson, K. (1901). Liii. on lines and planes of closest fit to systems of points in space. *The London, Edinburgh, and Dublin philosophical magazine and journal of science* 2, 559–572.
39. Greenacre, M., Groenen, P.J., Hastie, T., d’Enza, A.I., Markos, A., and Tuzhilina, E. (2022). Principal component analysis. *Nature Reviews Methods Primers* 2, 100.
40. Harrell, F.E., Califf, R.M., Pryor, D.B., Lee, K.L., and Rosati, R.A. (1982). Evaluating the yield of medical tests. *Jama* 247, 2543–2546.
41. Gélard, M., Richard, G., Pierrot, T., and Cournède, P.H. (2025). Bulkarnabert: Cancer prognosis from bulk rna-seq based language models. In *Proceedings of the 4th Machine Learning for Health Symposium* vol. 259 of *Proceedings of Machine Learning Research*. PMLR pp. 384–400.
42. Grattafiori, A., Dubey, A., Jauhri, A., Pandey, A., Kadian, A., Al-Dahle, A., Letman, A., Mathur, A., Schelten, A., Vaughan, A. et al. (2024). The llama 3 herd of models. *arXiv preprint arXiv:2407.21783*.

43. Ahlmann-Eltze, C., Huber, W., and Anders, S. (2024). Deep learning-based predictions of gene perturbation effects do not yet outperform simple linear methods. *BioRxiv* pp. 2024–09.
44. Moor, M., Banerjee, O., Abad, Z.S.H., Krumholz, H.M., Leskovec, J., Topol, E.J., and Rajpurkar, P. (2023). Foundation models for generalist medical artificial intelligence. *Nature* *616*, 259–265.
45. Kaissis, G.A., Makowski, M.R., Rückert, D., and Braren, R.F. (2020). Secure, privacy-preserving and federated machine learning in medical imaging. *Nature Machine Intelligence* *2*, 305–311.
46. Khalid, N., Qayyum, A., Bilal, M., Al-Fuqaha, A., and Qadir, J. (2023). Privacy-preserving artificial intelligence in healthcare: Techniques and applications. *Computers in Biology and Medicine* *158*, 106848.
47. Torkzadehmahani, R., Nasirigerdeh, R., Blumenthal, D.B., Kacprowski, T., List, M., Matschinske, J., Spaeth, J., Wenke, N.K., and Baumbach, J. (2022). Privacy-preserving artificial intelligence techniques in biomedicine. *Methods of information in medicine* *61*, e12–e27.
48. Siegel, R.L., Kratzer, T.B., Giaquinto, A.N., Sung, H., and Jemal, A. (2025). Cancer statistics, 2025. *Ca* *75*, 10.
49. Liu, H., Yang, H., Eduati, F., Pluim, J.P., and Veta, M. (2025). Adaptive prototype learning for multimodal cancer survival analysis. *arXiv preprint arXiv:2503.04643*.
50. Szałata, A., Hrovatin, K., Becker, S., Tejada-Lapuerta, A., Cui, H., Wang, B., and Theis, F.J. (2024). Transformers in single-cell omics: a review and new perspectives. *Nature methods* *21*, 1430–1443.
51. Yang, Z., Mitra, A., Kwon, S., and Yu, H. (2024). Clinicalmamba: A generative clinical language model on longitudinal clinical notes. *arXiv preprint arXiv:2403.05795*.
52. Beltagy, I., Peters, M.E., and Cohan, A. (2020). Longformer: The long-document transformer. *arXiv preprint arXiv:2004.05150*.
53. Kefeli, J., and Tatonetti, N. (2024). Tcga-reports: A machine-readable pathology report resource for benchmarking text-based ai models. *Mendeley Data*, V1, doi: 10.17632/hyg5xkznp.1. .
54. Chen, R.J., Ding, T., Lu, M.Y., Williamson, D.F., Jaume, G., Chen, B., Zhang, A., Shao, D., Song, A.H., Shaban, M. et al. (2025). Uni2-h-features. <https://huggingface.co/datasets/MahmoodLab/UNI2-h-features>. .
55. Kwon, W., Li, Z., Zhuang, S., Sheng, Y., Zheng, L., Yu, C.H., Gonzalez, J.E., Zhang, H., and Stoica, I. (2023). Efficient memory management for large language model serving with pagedattention. In *Proceedings of the ACM SIGOPS 29th Symposium on Operating Systems Principles*. pp. 611–626.
56. Lonsdale, J., Thomas, J., Salvatore, M., Phillips, R., Lo, E., Shad, S., Hasz, R., Walters, G., Garcia, F., Young, N. et al. (2013). The genotype-tissue expression (gtex) project. *Nature genetics* *45*, 580–585.



57. Consortium, E.P. et al. (2012). An integrated encyclopedia of dna elements in the human genome. *Nature* 489, 57.
58. Program, C.C.S., Abdulla, S., Aevermann, B., Assis, P., Badajoz, S., Bell, S.M., Bezzi, E., Cakir, B., Chaffer, J., Chambers, S. et al. (2025). Cz cellxgene discover: a single-cell data platform for scalable exploration, analysis and modeling of aggregated data. *Nucleic Acids Research* 53, D886–D900.
59. Pedregosa, F., Varoquaux, G., Gramfort, A., Michel, V., Thirion, B., Grisel, O., Blondel, M., Prettenhofer, P., Weiss, R., Dubourg, V. et al. (2011). Scikit-learn: Machine learning in python. *Journal of machine Learning research* 12, 2825–2830.
60. Pölsterl, S. (2020). scikit-survival: A library for time-to-event analysis built on top of scikit-learn. *Journal of Machine Learning Research* 21, 1–6.
61. Kaplan, E.L., and Meier, P. (1958). Nonparametric estimation from incomplete observations. *Journal of the American statistical association* 53, 457–481.